### Title

Single Amino Acid Substitution in the Vicinity of a Receptor-Binding Domain Changes Protein–Peptide Binding Affinity




### Journal

ACS Omega, 2(9)

### ISSN

2470-1343



### Authors

Malovichko, Galina
Zhu, Xiangdong



### Publication Date

2017-09-30

### DOI

10.1021/acsomega.7b00963

Peer reviewed

ACS OMEGA

Article

http://pubs.acs.org/journal/acsodf

# Single Amino Acid Substitution in the Vicinity of a Receptor-Binding Domain Changes Protein–Peptide Binding Affinity

Galina Malovichko and Xiangdong Zhu*

Department of Physics, University of California, Davis, California 95616, United States

**ABSTRACT:** Using a microarray-based assay, we studied how the substitution of amino acids in the immediate vicinity of the receptor-binding domain on a peptide affects its binding to a protein. Replicates of 802 linear peptides consisting of the variants of WT**HPQ**FAT and LQW**HPQ**AGK, GKFPIPLGKQSG, and NGQFQVWIPGAQK, different by one amino acid, were synthesized on a glass slide with a maskless photolithography. Using a microarray-compatible label-free optical sensor, we measured the binding curves of streptavidin with the synthesized peptides and extracted the streptavidin–peptide affinity constants. We found that (a) the substitution of one residue in the **HPQ** motif reduces the affinity constant $K_a$ from $10^8$ $M^{-1}$ by at least 3–4 orders of magnitude, with an exception of **HPM**; (b) substitution of the immediate flanking residue on the Gln side also causes the affinity to decrease by up to 3–4 orders of magnitude, depending on the substituting residue and the second-neighboring flanking residue; (c) substitution of the flanking residues on the His side has no significant effect on the affinity, possibly due to the strong binding of streptavidin to **HPQ**F and **HPQ**AG motifs. We also found that some of amino acid residues located close to the C-terminus (and the solid surface) improve the yield of peptide synthesis on a glass surface and can be exploited in the fabrication of peptide microarrays.

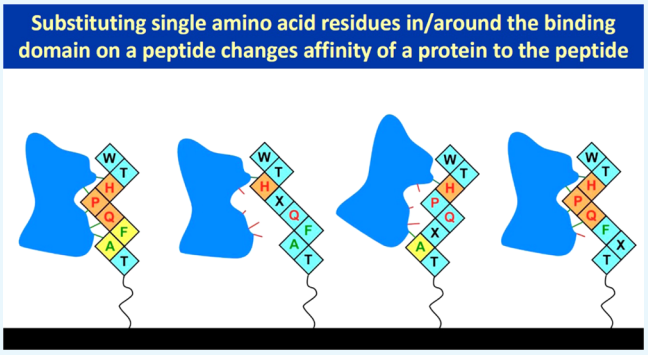


## INTRODUCTION

Understanding specific protein–peptide binding reactions and the corresponding structure–activity relationship (SAR) is a key to understanding and controlling protein–protein interactions and the associated signal pathways. Typically, through combinations of X-ray-based structural characterization and suitable affinity assays such as phage display,[1,2] one-bead-one-compound (OBOC) screening,[3] or synthetic peptide combinatorial library (SPCL),[4] one can identify a short sequence of amino acids on a peptide that serves as the receptor-binding domain (RBD) to a protein receptor, such that substituting any one amino acid in this sequence dramatically reduces the affinity between the receptor and the "modified" peptide. From the structural characterization,[5,6] one may reasonably ascertain how the geometric arrangement of the short sequence minimizes the Gibbs free energy through an optimal combination of the hydrogen bond formation, hydrophobic interaction, and peptic conformation. The length of such sequences varies from 3 to no more than 10 amino acids.[7,8] The roles of the flanking amino acid residues outside the RBD are less known, even though scattered experimental investigation on these residues indicate that they can have a significant positive or negative effect on the stability of protein–peptide complexes. The scarcity of such an information on the flanking residues is because (at least partly) the structural studies based on X-ray crystallography require stable protein–peptide complexes, making those peptides containing the same RBD but with "unfavorable" flanking residues inaccessible. This is also true for high-throughput screening assays such as phase display screening (routinely used to identify RBD in a peptide). Phage libraries may contain up to $10^8$–$10^{11}$ random sequences of amino acids, and phase display screening efficiently selects those peptides with high-affinity RBD.[1,9] Unfortunately, many (if not most) less-stable protein–peptide complexes with unfavorable flanking residues are not retained after panning or washing steps. In this regard, a high-throughput screening assay capable of following the association and dissociation of protein–peptide complexes in real time is desirable, as it can be employed to study systematically how the flanking amino acids outside an RBD on a peptide alter over a wide range the affinity between the protein and the peptide.

We here report a study of this kind using a combination of a photolithographically fabricated peptide microarray[10,11] and a compatible label-free optical sensor.[12,13] Although surface-plasmon-resonance (SPR)-based sensors have also been used to detect peptide microarrays, they are not yet compatible with photolithographically fabricated peptide microarrays.[14] For a model of protein–peptide complex that involves a well-defined RBD, we use streptavidin and synthesized peptides containing the **HPQ** motif. In particular, we examine the effect of altering single amino acid residue in WT**HPQ**FAT and LQW**HPQ**AGK on the affinity of the peptide variant to streptavidin. We will

**Received:** July 10, 2017
**Accepted:** August 24, 2017
**Published:** September 6, 2017

  

DOI: 10.1021/acsomega.7b00963
*ACS Omega* 2017, 2, 5445–5452

show that such an assay platform is useful for exploring the amino acid residues outside the RBD on a peptide for desirable as well as undesirable binding behaviors with a specific protein receptor. Our main finding is that the flanking residues up to the second neighbor can have a profound influence on the stability of a protein−peptide complex depending on the chemical identity and the structural attribute of the residues.

Peptide ligands to streptavidin are typically discovered through the phage library screening[1,15] or one-bead-one-compound (OBOC) screening,[3] followed by microcalorimetry and X-ray crystallographic studies of those with high affinity to protein. High-affinity ligands usually contain common motifs such as **HPQ** or **HPM** that bind to the same pocket to which biotin binds. The affinity of the **HPQ**-containing peptides has been shown, albeit in a limited way, to depend on the peptide conformation and the flanking residues.[3,5,6,15] For example, cyclic peptides are found to have affinity that is orders of magnitude higher than that of their linear counterparts due to a smaller entropic cost of the complex formation; the stability of streptavidin−**HPQ**F motif benefits from the hydrophobic interaction of the Phe residue with a likewise pocket on streptavidin; the binding to a **HPQ**N motif is assisted by Asn that forms extra H-bonds; whereas the streptavidin−**HPQ**GG complex is strengthened by the flexibility of the Pro−Pro sequence that facilitates an optimal peptide conformation.

To systematically explore the roles of flanking residues outside the RBD in a peptide, we use a real-time-detected synthetic peptide microarray platform. Although the throughput of $10^4$−$10^5$ per microarray is lower than that of the phage display or the OBOC screening assays, a lithographically fabricated peptide microarray has systematically modified and spatially registered peptide targets on a solid surface and enables the real-time detection of the protein−peptide association and dissociation during the reactions.[10−14] As a result, one can measure the peptide−protein affinity over a large dynamic range.

## MATERIALS AND PROCEDURES

**Microarray Synthesis and Layout.** The peptide microarray was synthesized with the maskless photolithography on glass slides by NimbleGen Inc.[11] The array consists of 4524 square features in a 52 × 87 arrangement. Each feature has a size of 108 × 108 $\mu m^2$. The gap between the features is also 108 $\mu$m. The entire microarray occupies a rectangular area of 11.1 × 18.7 $mm^2$. The feature size is chosen to ensure that the optical scanner (as described later) with a beam waist of 6 $\mu$m adequately resolves the features. In each feature, a variant of the following four peptides is synthesized: WT**HPQ**FAT (linear octapeptides), LQW**HPQ**AGK (linear nonapeptides), GKFPIPLGKQSG, and NGQFQVWIPGAQK. The last two peptides that do not contain the **HPQ** motifs are included as negative controls. In all of the cases, the C-terminus is at the right end of the sequence. Each variant is different from the original peptide by only one amino acid. Twenty natural amino acids are used to produce variants: Ala (A), Arg (R), Asn (N), Asp (D), Cys (C), Gln (Q), Glu (E), Gly (G), His (H), Ile (I), Leu (L), Lys (K), Met (M), Phe (F), Pro (P), Ser (S), Thr (T), Trp (W), Tyr (Y), and Val (V). For the original sequences, there are 65 replicates of WT**HPQ**FAT, 36 replicates of LQW**HPQ**AGK, 48 replicates of GKFPIPLGKQSG, and 52 replicates of NGQFQVWIPGAQK in the microarray. For variants, four replicates of each are synthesized at "random" locations in the microarray. In total, we have 802 distinct peptide variants, including the original sequences, and a total of 3537 peptide replicates of interest. The remaining features are included for alignment and fabrication controls.

**Streptavidin−Peptide Binding Reaction Procedures.** The glass slide bearing a peptide microarray is assembled with a custom fluidic chamber. The assembly is initially filled with 1× phosphate-buffered saline (PBS). To block the portion of the glass surface that has no fabricated features, we incubate the microarray in 2 $\mu$M of bovine serum albumin (BSA) solution in 1× PBS for 30 min. From the real-time binding curve measurements, we observe no evidence of BSA binding to the glass surface, indicating that the feature-free part of the glass surface is protected from nonspecific protein binding. For the reaction with streptavidin at room temperature, we incubate the microarray in fresh 1× PBS for 10 min to obtain a baseline for binding curves. We then replace the buffer with a 3 $\mu$M solution of streptavidin in 1× PBS and incubate the microarray under the flow condition for 60 min (the association phase); afterward, we replace the streptavidin solution with 1× PBS again and incubate under a flow condition for another 120 min (the dissociation phase).

**Microarray-Compatible Label-free Optical Detection.** To measure 4524 association−dissociation curves during the reactions of streptavidin with the synthetic peptide microarray having as many features, we use an ellipsometry-based label-free sensor (oblique-incidence reflectivity difference (OI-RD)) that has been described previously.[12] With this sensor, we measure the phase change in a reflected optical beam due to the presence of a biomolecular layer on a solid support during the reaction. Similar to a surface-plasmon-resonance (SPR) sensor, the phase change in OI-RD detection is proportional to the surface mass density $\Gamma$ of the biomolecular layer. The advantage of an OI-RD-based sensor is that it is compatible with microarray-based assays and capable of simultaneously detecting in real time tens of thousands reactions on a solid support.[13,14] The label-free feature of the detection also enables one to examine the quality of the microarray before the reaction for analysis and optimization.

Figure 1 shows the arrangement of an OI-RD-based detection of a peptide microarray in a fluidic chamber. The differential phase change $\delta$ is proportional to the surface mass density $\Gamma$ with a proportionality constant $C = -1.1 \times 10^4$ rad·$cm^2$/g, assuming that the volume mass density and refractive indices of peptides and protein probes are independent of the amino acid composition.[12]

We acquire an OI-RD image at 10 $\mu$m steps in both $x$ direction and $y$ direction. Figure 2a shows the image of a fresh peptide microarray in 1× PBS before the reaction. Four replicates of a peptide variant are highlighted. For the end points of the streptavidin reactions with the synthesized peptides, we capture the OI-RD images of the microarray before the association phase and after the dissociation phase of the reaction. We take the difference as the measure of captured streptavidin or, more precisely, nondissociated streptavidin−peptide complexes after 2 h. This is shown in Figure 2b. It reveals the amount of captured streptavidin by those peptides with sufficiently high affinity.

For the association−dissociation curve measurements, we record the signals only from the center of each feature and a point midway between the two neighboring features (a reference pixel). We take the difference between the signal from a peptide feature and the average of the signals from the two neighboring reference pixels as one time point. Each time



DOI: 10.1021/acsomega.7b00963
ACS Omega 2017, 2, 5445−5452

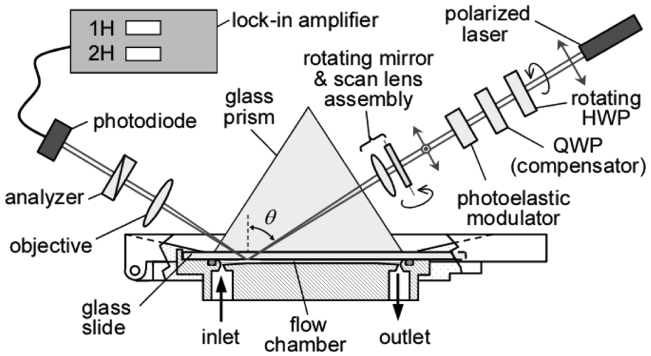


**Figure 1.** Scanning OI-RD microscope for detecting 4524 protein–peptide reactions in real time. A polarized laser beam passes a photoelastic modulator and a phase shifter that alter the beam polarization periodically and statically. A lens assembly focuses and scans the polarization-modulated beam across the surface of the microarray along the *y* direction, whereas a translation stage holding the fluid chamber moves along the *x* direction to complete the two-dimensional scan. The beam is total internally reflected from the surface and then passes through an analyzer before being detected with the photodiode. The ratio of the first harmonic (1H) of the modulation frequency in the photocurrent to the second harmonic (2H) is used to extract the differential phase $\delta$. The latter is proportional to the surface mass density of the biomolecular layer.

step takes 18 s. By scanning the microarray repeatedly every 18 s, we acquire the association–dissociation curves for all of the 4254 peptide variants and controls; 1393 of them are variants of WT**HPQ**FAT and LQW**HPQ**AGK. Figure 3 shows the association–dissociation curves for the three variants of LQW**HPQ**AGK. For each of the 802 peptide variants, regardless of whether it forms a stable complex with streptavidin that survives the dissociation phase, we have a set of association–dissociation curves acquired from its replicates. We globally fit the curve set to one-site Langmuir reaction model. From the fit, we obtain the affinity constant given by $K_a = k_{on}/k_{off}$. We use $K_a$ instead of the end points of the reaction in our analysis because $K_a$'s obtained from the binding curve sets have a much larger dynamic range and include those reactions with large dissociation rate constants and are, thus, easily missed in the differential image (Figure 2b).

## RESULTS

Figure 4 displays the affinity constants of 153 variants of WT**HPQ**FAT with streptavidin. There are eight panels, and each panel displays $K_a$ of the 20 variants that are different by one amino acid at a fixed location on WT**HPQ**FAT. For example, the third panel shows the affinity constants of those peptides that have the form of WT(X)**PQ**FAT, with X being one of the 20 natural amino acids. Figure 5 displays the affinity

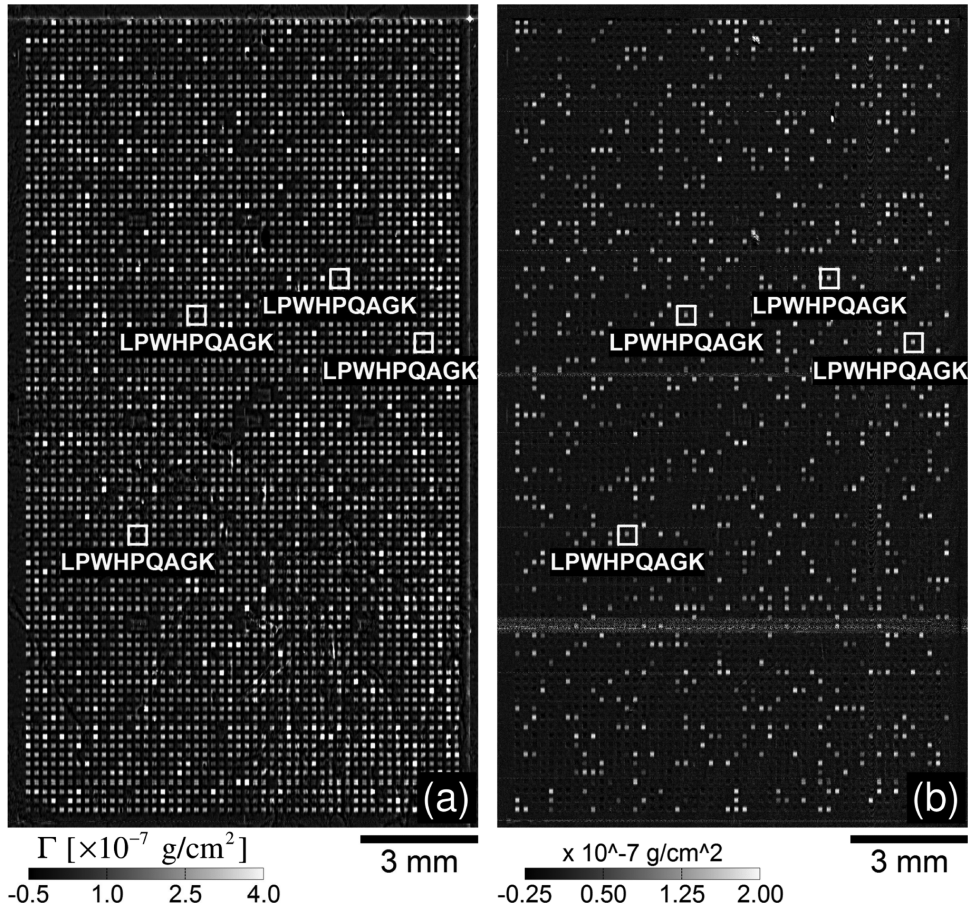


**Figure 2.** (a) Image in surface mass density of the peptide microarray in 1× PBS acquired with an OI-RD microscope before the reaction. Yellow boxes show four replicates of LPW**HPQ**AGK. (b) Change in the surface mass density as a result of the reaction with streptavidin obtained by taking the difference between the image acquired after the dissociation phase and the image obtained before the association phase. The scale of (b) is expanded by a factor of 2 from that of (a).



DOI: 10.1021/acsomega.7b00963
*ACS Omega* 2017, 2, 5445–5452

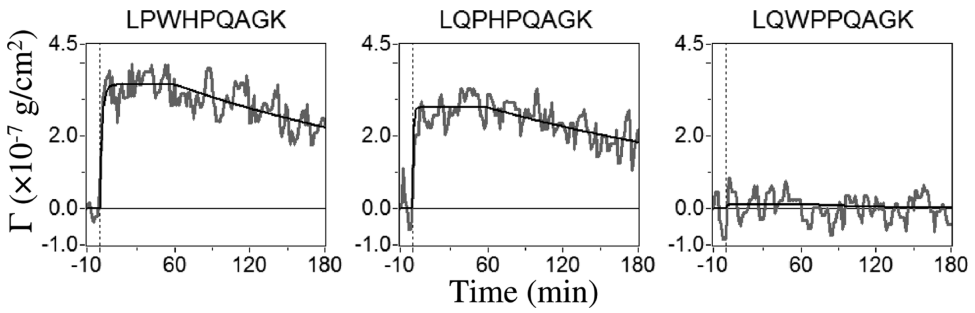


**Figure 3.** Association−dissociation (binding) curves of streptavidin to variants of LQW**HPQ**AGK. Vertical dashed lines mark the start and the end of a 60 min association phase, preceded by a 10 min baseline, and followed by a 120 min dissociation phase. Solid black lines show fitting to one-site Langmuir model.

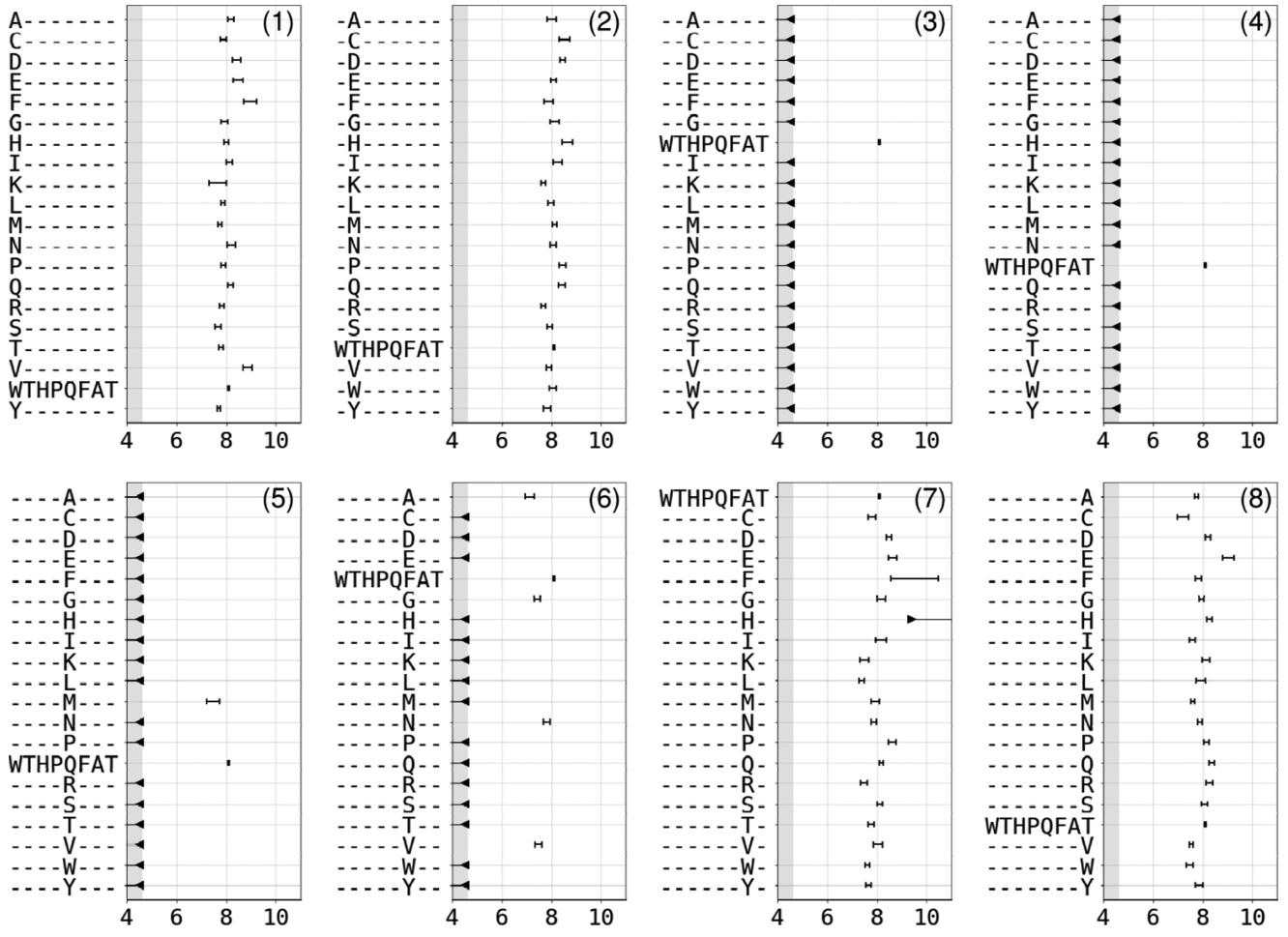


**Figure 4.** Affinity constants of 153 variants of WT**HPQ**FAT to streptavidin. The unit for the horizontal axes is $\log_{10}(K_a)$, with $K_a$ in $M^{-1}$. Panel (1) lists those for (X)T**HPQ**FAT; panel (2) for W(X)**HPQ**FAT; panel (3) for WT(X)**PQ**FAT; panel (4) for WT**H**(X)**Q**FAT; panel (5) for WT**HP**(X)FAT; panel (6) for WT**HPQ**(X)AT; panel (7) for WT**HPQ**F(X)T; and panel (8) for WT**HPQ**FA(X). X is one of the 20 natural amino acids.

constants of 172 variants of LQW**HPQ**AGK, and there are nine panels for as many residue locations on the peptide. The error bar on each data point is the variance obtained from four or more duplicate targets of the same peptide sequence. When the captured streptavidin is below the detection limit in the present study, only the upper bound is reported. For a few peptide ligands, the dissociation rates $k_{off}$ are below the detection limit; in these cases, we report only the lower bound of $K_a$.

When a peptide sequence is synthesized on a solid support, the motif of interest is purposely located at a distance from the surface through a spacer (in this case, a few nonfunctional amino acids) to minimize the effect of the surface. Figures 4 and 5 show that as few as two to three 3 amino acid residues are sufficient to buffer the motif from the presence of the solid surface, indicating that the flanking residues beyond the second neighbor do not have a significant effect on the peptide−protein binding. We now examine the details revealed by these two figures.

### HPQ is the Receptor-Binding Domain (RBD) of a Linear Peptide for Complex Formation with Streptavi-



DOI: 10.1021/acsomega.7b00963
ACS Omega 2017, 2, 5445−5452

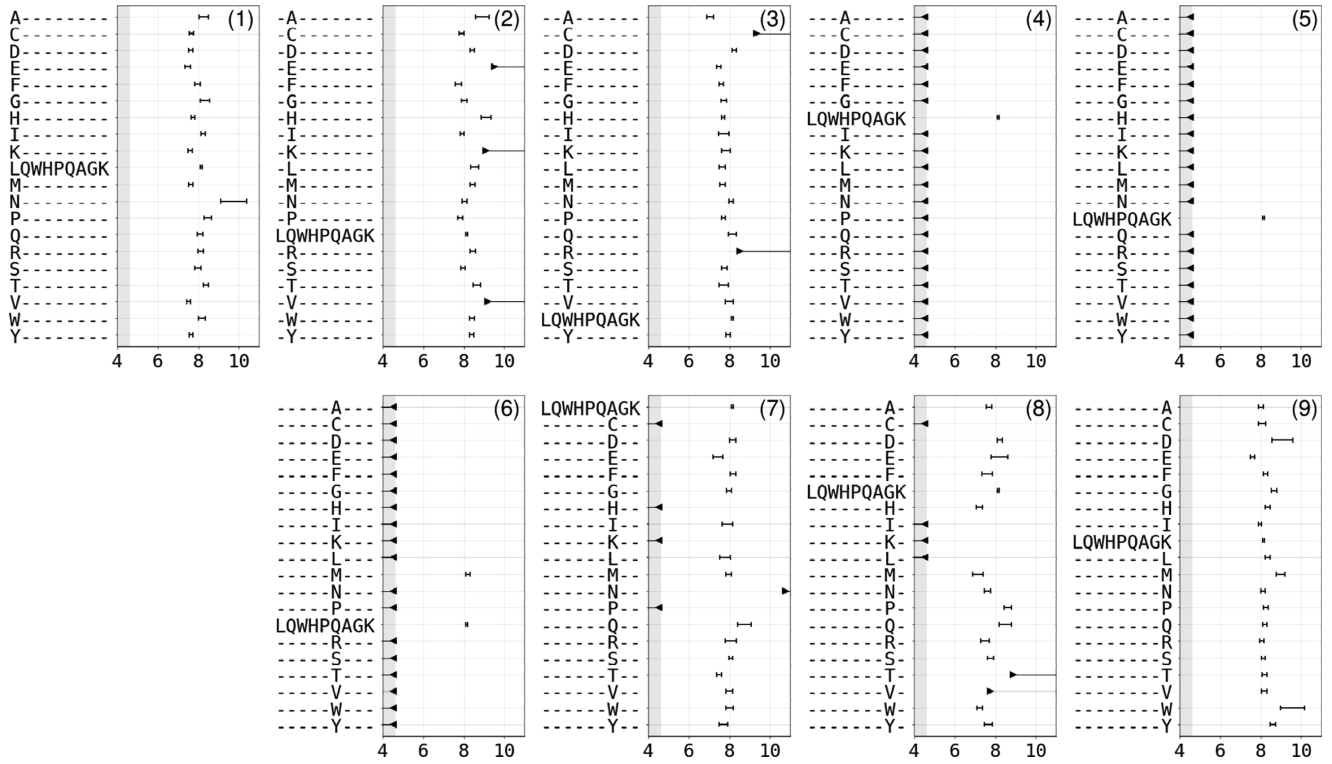

**Figure 5.** Affinity constants of 172 variants of LQW**HPQ**AGK to streptavidin. The unit for the horizontal axes is $\log_{10}(K_a)$, and $K_a$ is in $M^{-1}$. Panel (1) lists those for (X)QW**HPQ**AGK; panel (2) for L(X)W**HPQ**AGK; panel (3) for LQ(X)**HPQ**AGK; panel (4) for LQW(X)**PQ**AGK; panel (5) for LQW**H**(X)**Q**AGK; panel (6) for LQW**HP**(X)AGK; panel (7) for LQW**HPQ**(X)GK; panel (8) for LQW**HPQ**A(X)K; and panel (9) for LQW**HPQ**AG(X). X is one of the 20 natural amino acids.

**din.** One can immediately see that the affinity constants for XX-**HPQ**FAT, XXX-**HPQ**AGK, WT**HPQ**FA-X, and LQW**HPQ**AG-X are essentially the same, namely, $K_a \approx 10^8$ $M^{-1}$. As a result, the latter is typical of the high-affinity linear peptide ligands to streptavidin on a solid support. From panels (3)−(5) in Figure 4 and from panels (4)−(6) in Figure 5, we can conclude that the substitution of any one residue in the **HPQ** motif (except for **HPM**) causes the affinity constant to decrease from $10^8$ $M^{-1}$ by at least 3 orders of magnitude, that is, below $10^5$ $M^{-1}$ (the detection limit under the current assay condition). This reaffirms what is known in the literature that **HP**(**Q**/M) are necessary for a peptide to bind strongly to streptavidin at the pocket where a biotin binds.

**First- and Second-Neighboring Flanking Residues Adjacent to Gln of HPQ have Profound Effects on Formation of Peptide−Streptavidin Complexes.** From panels (6) and (7) of Figure 4 and panels (7) and (8) of Figure 5, we see that $K_a$ begins to significantly deviate from $10^8$ $M^{-1}$ when one of the first- and second-neighboring flanking residues on the Gln side is replaced, namely, for WT**HPQ**(X ≠ F)AT, WT**HPQ**F(X ≠ A)T, LQW**HPQ**(X ≠ A)GK, and LQW**HPQ**A(X ≠ G)K.

Specifically, panel (6) in Figure 4 illustrates the profound influence of the first flanking residue on the Gln side for the stability of peptide−streptavidin complexes as only 5 out of 20 WT**HPQ**(X)AT (i.e., WT**HPQ**(F, A, G, N, V)AT) have the affinity constants over $10^7$ $M^{-1}$, whereas the remaining 15 WT**HPQ**(X)AT have their affinity constants less than $10^5$ $M^{-1}$.

Panel (7) in Figure 5 and panel (6) in Figure 4 collectively reveal almost as important an effect of the second flanking residue on the stabilizing linear peptide−streptavidin complexes. By replacing the second flanking residue from A to G, 15 out of 20 LQW**HPQ**(X)GK (e.g., LQW**HPQ**SGK) form stable complexes with streptavidin, with the affinity constants in the range of $10^7$ $M^{-1}$. Only LQW**HPQ**(C, H, K, P)GK have drastically reduced affinity to streptavidin—under $10^5$ $M^{-1}$. The combination of these two panels suggest that regardless of the residues at other locations, linear peptides containing **HPQ**(C, H, K, P) do not form stable complexes with streptavidin, whereas linear peptides containing **HPQ**(F, G, N, V) do. The role of the second-neighboring flanking residue is further illustrated in panel (8) in Figure 5. When the second-neighboring flanking residue is one of C, I, K, and L, the linear peptides with **HQP**A motifs do not form stable complexes with streptavidin.

**First- and Second-Neighboring Flanking Residues Adjacent to His of the HPQ Motif Have Little Effect on Stable Complex Formation of Streptavidin with Peptides Containing HPQF and HPQAG.** Panels (1) and (2) in Figure 4 show that the substitution of the first and second flanking residues on the His side of the **HPQ** motif does not significantly change the affinity of (XX)**HPQ**FAT. Similarly, panels (1) and (2) in Figure 5 show that the substitution of the first and second flanking residues on the His side of the **HPQ** motif has little effect on the affinity of L(XX)**HPQ**AGT. One of the two possibilities is at work here: the substitution of the flanking residues on the His side generally has no substantial effects on the affinity of a **HPQ**-containing linear peptide to streptavidin, or **HPQ**F and **HPQ**AG motifs provide the needed stability of a linear peptide with the protein so that other residues, including the flanking residues on the His side, are rendered insignificant in affecting the complex formation. From the studies reported by Giebel et al.[15] and Lam et al.,[3] both possibilities seem to be at work.



DOI: 10.1021/acsomega.7b00963
*ACS Omega* 2017, 2, 5445−5452

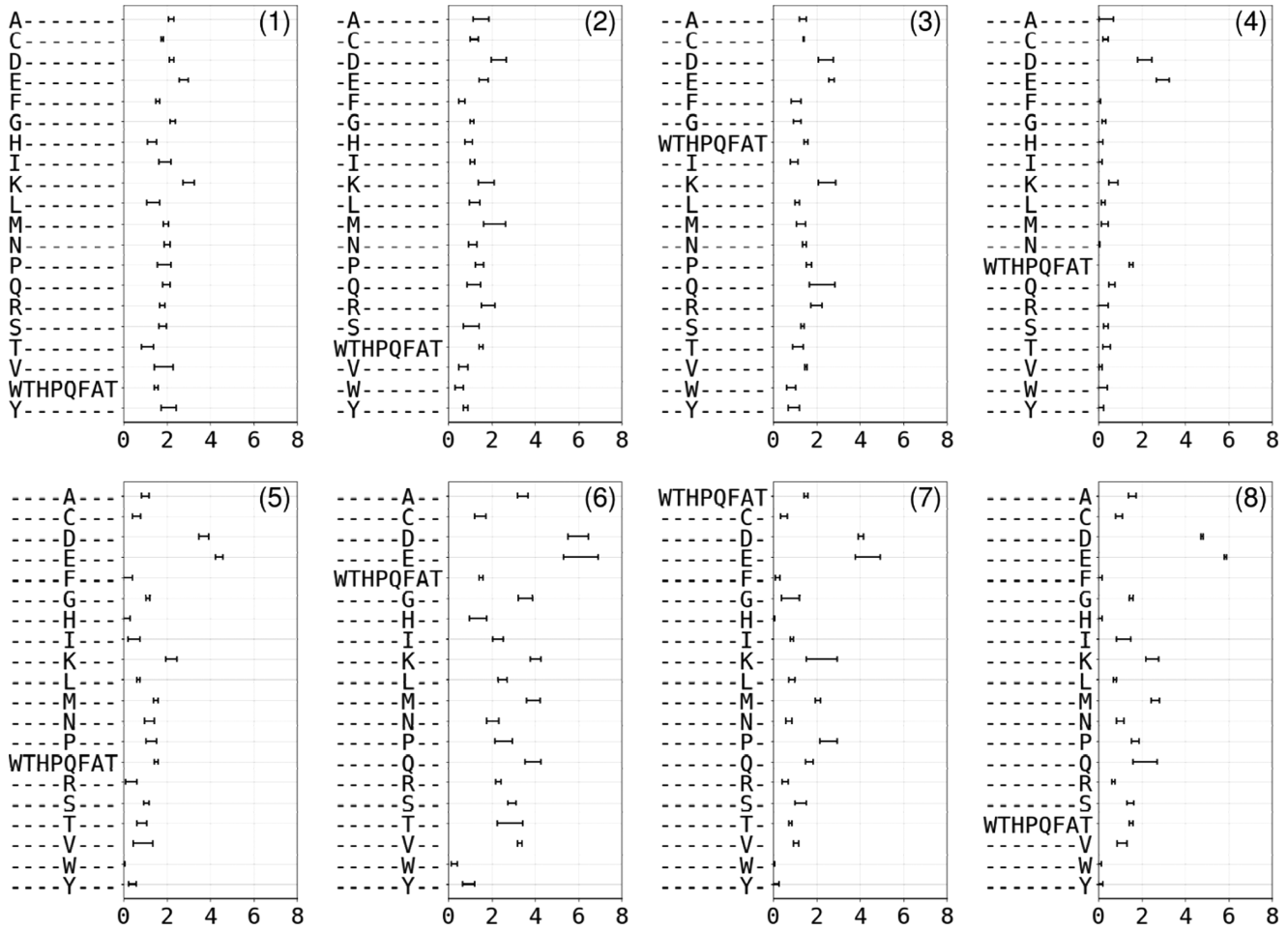


**Figure 6.** Surface mass densities (in unit of $10^{-7}$ g/cm$^2$) of 153 variants of WT**HPQ**FAT synthesized on a glass slide. Panel (1): (X)T**HPQ**FAT; panel (2): W(X)**HPQ**FAT; panel (3): WT(X)**PQ**FAT; panel (4): WT**H**(X)**Q**FAT; panel (5): WT**HP**(X)FAT; panel (6): WT**HPQ**(X)AT; panel (7):WT**HPQ**F(X)T; and panel (8): WT**HPQ**FA(X). X is one of the 20 natural amino acids.

## DISCUSSION

The roles of flanking residues outside the **HPQ** motif in the complex formation of peptides with streptavidin have been reported and discussed in the literature.[5,6,15] By screening the cyclic hexa/hepta/octapeptide phage libraries, Giebel and co-workers found that (a) isolated peptides (in solution phase as opposed to those attached to a substrate such as a solid support) that strongly bind to streptavidin all have an **HPQ** motif; (b) the **HPQ** motif is almost always immediately adjacent to the N-terminal cysteine; and (c) these cyclic peptide ligands have either **HPQ**(G, F, V, N) motifs or **HPQ**(SG) motif. For hexapeptides, only C**HPQ**FC is found after three rounds of biopanning. The fact that cyclic hepta- and octapeptide ligands almost always have the **HPQ** motif close to the N-terminal was attributed by these authors to the constraint on the short cyclic peptides and the need for an optimal display of **HPQ** side chains. In the light of our present study, it seems equally likely (if not more so) that cyclic hepta- and octapeptide ligands need to have suitable flanking residues adjacent to the Gln side to have peptide−streptavidin complexes. This can be accommodated only if the **HPQ** sequence is close to the N-terminal cysteine, making room for flanking residues such as F, G, V, N, and SG on the Gln side. This explanation is consistent with our observation that linear peptides with **HPQ**(G, F, V, N) motif or **HPQ**(SG) motif and yet no constraint brought about by the cyclic structure also bind to streptavidin with high affinity. It is also consistent with our observation that flanking residues on the His side seem less important than the residues on the Gln side in stabilizing the complexes.

Specific to our present microarray-based study, we found that linear peptides containing **HPQ**(F, G, N, V) motifs form stable complexes with streptavidin as their cyclic counterparts. In addition, we found that the linear peptides containing **HPQ**(A) motif also form stable complexes with streptavidin—a motif not reported in previous studies. Furthermore, similar to the observation by Giebel et al. on short cyclic peptides,[15] we found that linear peptides containing **HPQ**(SG) motif form stable complexes with streptavidin as well. More importantly, we discovered the reason for the high affinity of **HPQ**(SG) motif: as the second flanking residue on the Gln side, the Gly residue acts to stabilize the complex formation of streptavidin with **HPQ**SG and nine other linear peptides with **HPQ**(D, E, I, L, M, N, Q, R, T, W, Y)G motifs. It seems that **HPQ**F and **HPQ**AG motifs sufficiently stabilize the peptide−streptavidin complexes, rendering the flanking residues on the His side irrelevant. In the absence of suitable flanking residues on the Gln side, Lam et al. found 12 **HPQ**-containing linear pentapeptide ligands to streptavidin with flanking residues (MY, RE, IQ, GN, TV, IG, WM, GA, PL, AI, AA, and TP) only on the His side.[3] Their observation indicates that the stabilizing



DOI: 10.1021/acsomega.7b00963
*ACS Omega* 2017, 2, 5445−5452

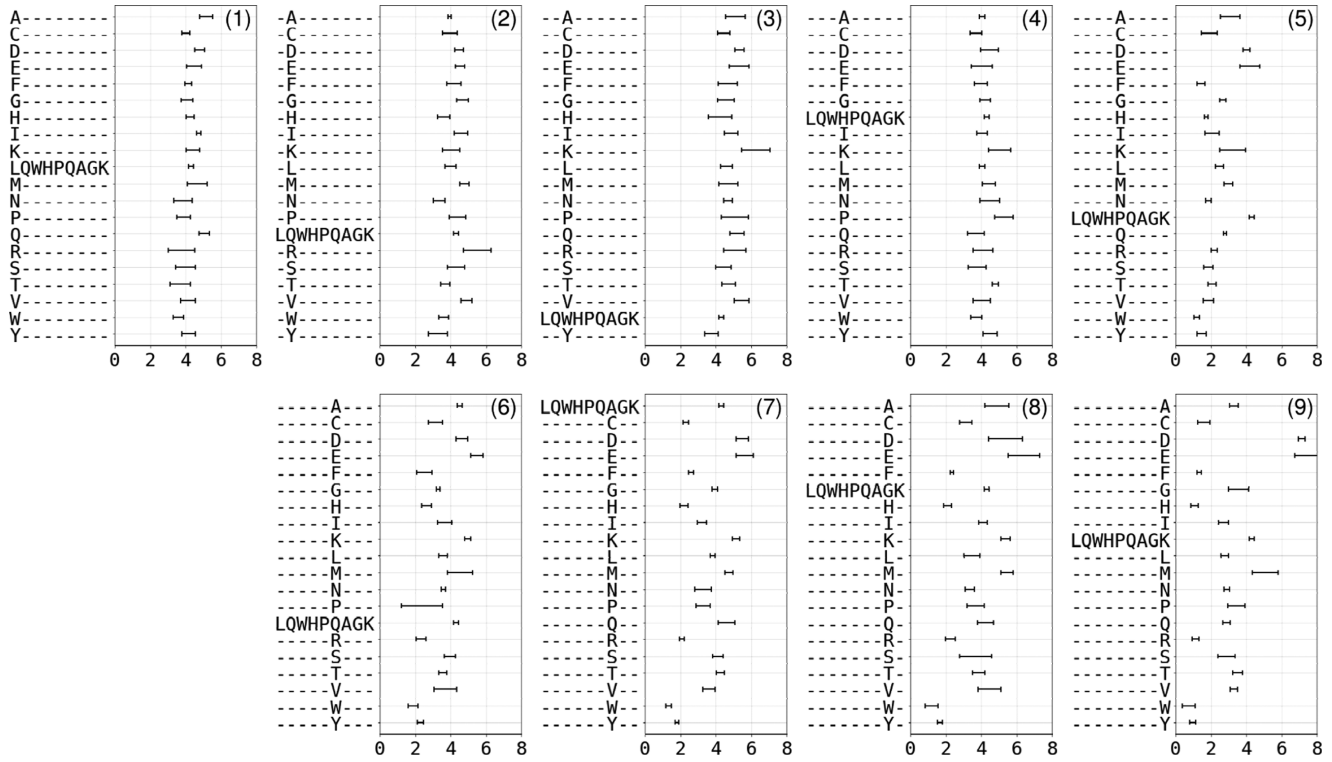

**Figure 7.** Surface mass densities (in unit of $10^{-7}$ g/cm$^2$) of 172 variants of LQW**HPQ**AGK synthesized on a glass slide. Panel (1): (X)QW**HPQ**AGK; panel (2): L(X)W**HPQ**AGK; panel (3): LQ(X)**HPQ**AGK; panel (4): LQW(X)**PQ**AGK; panel (5): LQW**H**(X)**Q**AGK; panel (6): LQW**HP**(X)AGK; panel (7): LQW**HPQ**(X)GK; panel (8): LQW**HPQ**A(X)K; and panel (9): LQW**HPQ**AG(X). X is one of the 20 natural amino acids.

effect of these flanking residues on the His side (not encountered in our present study) is also significant.

**Constraints on Linear Peptides Synthesized on a Solid Support Increases the Affinity to Streptavidin Due to Reduced Entropy Cost.** Affinity constants $K_a$ for the majority of synthesized linear peptides that bind to streptavidin are between $10^7$ and $10^9$ $M^{-1}$. This means that the equilibrium dissociation constants $K_D$ are between a few nM and 100 nM, much higher than those for isolated **HPQ**-containing linear peptides with same flanking residues. This is expected, as constraints on the conformation of linear peptides synthesized on a solid support reduce the entropy cost when forming complexes with streptavidin and thus increase affinity constants from those for solution-phase linear peptides.[15]

**Mechanisms for Complex Formation of Streptavidin with Linear Peptides Having Various HPQ-Containing Motifs.** With limited X-ray-based structural data available, it is difficult and premature to draw a general rule on how flanking residues help to stabilize peptide−streptavidin complexes. Yet, based on the work of Katz,[5] we make an attempt here to propose a few likely scenarios as guides to understand the protein−peptide complex formation in general. On the role of the first flanking residue, it seems that (a) the **HPQ**G motif stabilizes the linear peptide−protein complex by the Gly main chain amide forming an intrapeptide hydrogen bond with the His main chain carbonyl, thus defining a favorable type I $\beta$-turn in the peptide, as found by Katz in the C**HPQ**GPPC−streptavidin complex; (b) the **HPQ**N motif stabilizes the complexes by Asn residue forming additional direct and water-mediated hydrogen bonds with the protein, as found in FS**HPQ**NT−streptavidin complex by Katz; (c) **HPQ**(F,V,A) motifs achieve the same feat by (F,V,A) enacting hydrophobic interaction with a likewise pocket on the protein, as in C**HPQ**FC−streptavidin complexes. Because the hydrophobic side chain on Ala is much smaller, its stabilizing effect is expected to be somewhat reduced. This would explain why linear peptides with **HPQ**A(C, I, K, L) motifs have a much lower affinity to streptavidin than those with **HPQ**F(C, I, K, L) motifs.

The roles of the second-neighboring flanking residues on the formation of peptide−streptavidin complexes have not been studied before. As such, there is no direct or indirect X-ray structural data available that would shed light on what they bring to the complex. Yet, the influence of these flanking residues is clearly not negligible. The positive effect is illustrated in panel (6) of Figure 4 and panel (7) of Figure 5: the Gly residue stabilizes most peptides with **HPQ**(X)G motifs with streptavidin, whereas the Ala residue does a much poorer job for peptides with **HPQ**(X)A motifs. On the other hand, the fact that linear peptides with **HPQ**A(C, I, K, L) motifs have affinities at least 3 orders of magnitude less than those with **HPQ**A(X, X ≠ C, I, K, L) motifs demonstrates the destabilizing effect of C, I, K, and L as the second-neighboring flanking residues.

Finally, we should note that the OI-RD image of a peptide microarray before the reaction enables us to examine the quality of the array. Figure 2a shows that the surface mass density of the synthesized peptides varies within a square feature and from one feature to another. This image ensures that the negative "hit" is not due to the absence of target materials. In further analyzing the image, we notice that the sequence of a peptide, particularly the amino acid residues close to the C-terminus, affects the efficiency of the synthesis and, in turn, the peptide target number density. Figure 6 shows the



DOI: 10.1021/acsomega.7b00963
ACS Omega 2017, 2, 5445−5452

surface mass densities of the variants of WT**HPQ**FAT and Figure 7 shows the variants of LQW**HPQ**SGK. We find that some residues close to the C-terminus, and thus the solid surface, lead to significantly higher peptide densities, whereas some others do just the opposite. For example, the linear peptides with Asp (D) and Glu (E) having negatively charged side chains and being close to the C-terminus have significantly higher surface number densities than the linear peptides of otherwise same sequences. In contrast, Trp (W) and Tyr (Y), having bulky aromatic side chains, have significantly smaller surface number densities when they are close to the C-terminus. These tendencies hold true even when these residues are farther away from the C-terminus. One can then use the residues such as D, E, W, and Y to optimize the number density of synthesized peptides for subsequent binding assays.

## CONCLUSIONS

The quest for understanding protein−protein interactions and devising peptide-based drugs to modulate these interactions calls for the identification and functional characterization of key receptor-binding domains (RBD) on a peptide.[9,16,17] Our present study, in combination with earlier studies by others, shows that the flanking residues outside an RBD, at least up to the second neighbors, are crucial in stabilizing or destabilizing the peptide−protein complex formation and their roles should be systematically investigated and explored. A photolithographically synthesized peptide microarray on a glass slide detected with a compatible label-free sensor is an efficient assay platform for such an investigation and exploration. If it generally holds that only up to the second neighboring flanking residues are important in peptide−protein binding, one can then explore residues at positions beyond the second neighbors that add other desirable attributes of drug candidates, such as resistance against proteolysis, circulation time, plasma membrane penetration, and low toxicity,[9,16,17] or simply enable efficient and controllable synthesis on a solid support.[11]

## AUTHOR INFORMATION

### Corresponding Author

*E-mail: xdzhu@physics.ucdavis.edu.

### ORCID

Xiangdong Zhu: 0000-0002-6470-8054

### Notes

The authors declare no competing financial interest.

## ACKNOWLEDGMENTS

The authors thank NimbleGen Inc. for supplying the peptide microarrays used in this work.

## REFERENCES

(1) Devlin, J. J.; Panganiban, L.; Devlin, P. Random peptide libraries: a source of specific protein binding molecules. *Science* **1990**, *249*, 404−406.

(2) Fukunaga, K.; Taki, M. Practical tips for construction of custom peptide libraries and affinity selection by using commercially available phase display cloning systems. *J. Nucleic Acids* **2012**, *2012*, No. 295719.

(3) Lam, K. S.; Salmon, S. E.; Hersh, E. M.; Hruby, V. J.; Kazmierski, W. M.; Knapp, R. J. A new type of synthetic peptide library for identifying ligand-binding activity. *Nature* **1991**, *354*, 82−84.

(4) Houghten, R. A.; Pinilla, C.; Blondelle, S. E.; Appel, J. R.; Dooley, C. T.; Cuervo, J. H. Generation and use of synthetic peptide combinatorial libraries for basic research and drug discovery. *Nature* **1991**, *354*, 84−86.

(5) Katz, B. A. Binding to protein targets of peptidic leads discovered by phage display: crystal structures of streptavidin-bound linear and cyclic peptide ligands containing the HPQ sequence. *Biochemistry* **1995**, *34*, 15421−15429.

(6) Katz, B. A. Structural and mechanistic determinants of affinity and specificity of ligands discovered or engineered by phase display. *Annu. Rev. Biophys. Biomol. Struct.* **1997**, *26*, 27−45.

(7) Tompa, P.; Davey, N. E.; Gibson, T. J.; Babu, M. M. A million peptide motifs for the molecular biologist. *Mol. Cell* **2014**, *55*, 161−169.

(8) Shiba, K. Natural and artificial peptide motifs: their origins and the application of motif-programming. *Chem. Soc. Rev.* **2010**, *39*, 117−126.

(9) McGregor, D. P. Discovering and improving novel peptide therapeutics. *Curr. Opin. Pharmacol.* **2008**, *8*, 616−619.

(10) Shin, D.-S.; Lee, K.-N.; Yoo, B.-W.; Kim, J.; Kim, M.; Kim, Y.-K.; Lee, Y.-S. Automated maskless photolithography system for peptide microarray synthesis on a chip. *J. Comb. Chem.* **2010**, *12*, 463−471.

(11) Albert, T.; Richmond, T.; Rodesch, M.; Stengele, K.-P; Buehler, J.; Ott, M. Methods for Synthesis of an Oligopeptide Microarray. U.S. Patent US20120238477 A1, 2013.

(12) Landry, J. P.; Fei, Y.; Zhu, X. D. Simultaneous measurement of 10,000 protein-ligand affinity constants using microarray-based kinetic constant assays. *Assay Drug Dev. Technol.* **2012**, *10*, 250−259.

(13) Landry, J. P.; Ke, Y.; Yu, G.-L.; Zhu, X. D. Measuring affinity constants of 1,450 monoclonal antibodies to peptide targets with a microarray-based label-free assay platform. *J. Immunol. Methods* **2015**, *417*, 86−96.

(14) Cherif, B.; Roget, A.; Villiers, C. L.; Calemczuk, R.; Leroy, V.; Marche, P. N.; Livache, T.; Villiers, M. Clinically related protein-peptide interactions monitored in real time on novel peptide chips by surface plasmon resonance imaging. *Clin. Chem.* **2006**, *52*, 255−262.

(15) Giebel, L. B.; Cass, R.; Milligan, D. L.; Young, D.; Arze, R.; Johnson, C. Screening of cyclic peptide phage libraries identifies ligands that bind streptavidin with high affinities. *Biochemistry* **1995**, *34*, 15430−15435.

(16) Sato, A. K.; Viswanathan, M.; Kent, R. B.; Wood, C. R. Therapeutic peptides: technological advances driving peptides into development. *Curr. Opin. Biotechnol.* **2006**, *17*, 638−643.

(17) Vlieghe, P.; Lisowski, V.; Martinez, J.; Khrestchatisky, M. Synthetic therapeutic peptides: science and market. *Drug Discovery Today* **2010**, *15*, 40−56.



DOI: 10.1021/acsomega.7b00963
*ACS Omega* 2017, 2, 5445−5452